

APPARATUS AND DEMONSTRATION NOTES

Jeffrey S. Dunham, *Editor*

Department of Physics, Middlebury College, Middlebury, Vermont 05753

This department welcomes brief communications reporting new demonstrations, laboratory equipment, techniques, or materials of interest to teachers of physics. Notes on new applications of older apparatus, measurements supplementing data supplied by manufacturers, information which, while not new, is not generally known, procurement information, and news about apparatus under development may be suitable for publication in this section. Neither the *American Journal of Physics* nor the Editors assume responsibility for the correctness of the information presented. Submit materials to Jeffrey S. Dunham, *Editor*.

A classroom experiment to demonstrate ferroelectric hysteresis

M. Dawber, I. Farnan, and J. F. Scott

Earth Sciences Department, Downing Street, University of Cambridge, Cambridge CB2 3EQ, United Kingdom

(Received 19 July 2002; accepted 24 January 2003)

We have developed a classroom experiment suitable for undergraduate students in which they fabricate a ferroelectric capacitor from potassium nitrate and then observe the electrical behavior as the film is cooled through its transition temperature. The experiment can be carried out using a capacitance bridge that is simple to construct and inexpensive. The experiment gives students a hands-on experience with ferroelectric phenomena, a subject of considerable interest from both a fundamental and a technological standpoint. © 2003 American Association of Physics Teachers.

[DOI: 10.1119/1.1561271]

I. INTRODUCTION

There are at least three systems in nature that exhibit hysteretic responses to driving forces: ferromagnets, ferroelectrics, and ferroelastics. (The latter are materials that have hysteresis in their stress-strain relationships.¹) Of the three systems, only ferromagnets are usually the subject of undergraduate laboratory experiments. A ferroelectric is a material in which an electric dipole moment is present even in the absence of an external field. This typically occurs as a result of a change in the crystal structure so that the centers of positive and negative charge in the crystal do not coincide. A brief section on ferroelectric phase transitions is included in Kittel's textbook² and more detailed information can be obtained from Fatuzzo and Merz.³ Normally it is difficult to demonstrate ferroelectricity in the classroom laboratory as the coercive fields of most materials are of the order of kV/cm, making experiments on bulk ferroelectrics potentially dangerous and unsuitable for students. Ferroelectrics in thin film form, on the other hand, may be switched with a few volts and there is now both production of and research on nonvolatile memories based on ferroelectric thin films.⁴ Typically, however, thin films are deposited in expensive chemical vapor deposition or pulsed-laser deposition machines, making the fabrication of thin films by students as part of a teaching experiment impractical. We present here an experiment in which students make and characterize a ferroelectric thin film capacitor. The method outlined here is both safe and inexpensive.

Potassium nitrate is a material with a ferroelectric phase (phase III) which in bulk form is stable only between 115 and 125 °C, but is metastable at room temperature. It has

been found that when KNO₃ is made as a thin film, the lower temperature limit of the ferroelectric phase is lowered, and it can be stable at room temperature.⁵ Phase diagrams for bulk KNO₃⁶ and for thin films⁷ are shown in Figs. 1 and 2, respectively. In bulk the phase transition is a re-entrant phase transition, i.e., it can be reached only on cooling and not by heating. This is because the ferroelectric phase is narrower than the thermal hysteresis.

Potassium nitrate is not used for commercial applications because the challenges of fabricating capacitors have proven too difficult. KNO₃ readily absorbs water from the atmosphere, thereby severely degrading its ferroelectric properties. The main materials used today for ferroelectric memories are lead zirconate titanate and strontium bismuth tantalate. Because potassium nitrate melts at about 330 °C it is quite straightforward to melt the powder and then cool it to form a thin film in which hysteresis properties may be measured with an acceptably low voltage. We have designed an experiment to fabricate and measure the properties of a KNO₃ capacitor that is suitable for an undergraduate course. This experiment was run successfully this year as part of the first year course "Materials and Mineral Sciences 1A," a shared course between the Department of Earth Sciences and the Department of Material Sciences at the University of Cambridge.

II. SAWYER-TOWER CIRCUIT

The standard circuit used to measure a ferroelectric hysteresis loop is the Sawyer-Tower circuit.⁸ Our implementation of this circuit is shown in Fig. 3.

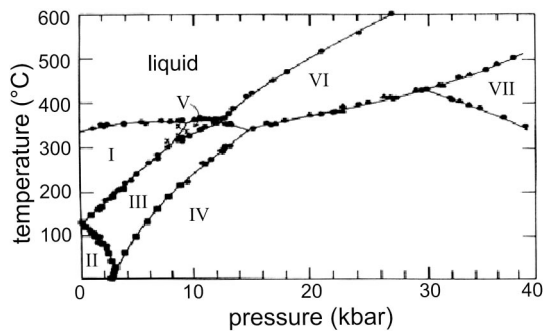


Fig. 1. Phase diagram for bulk KNO_3 with temperature as a function of hydrostatic pressure.

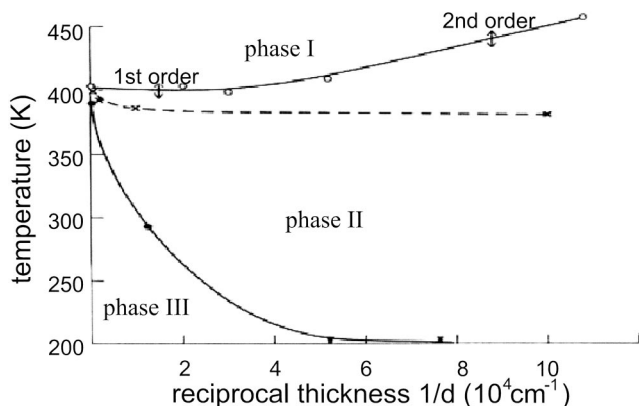


Fig. 2. Phase diagram for KNO_3 thin films with temperature as a function of reciprocal thickness.

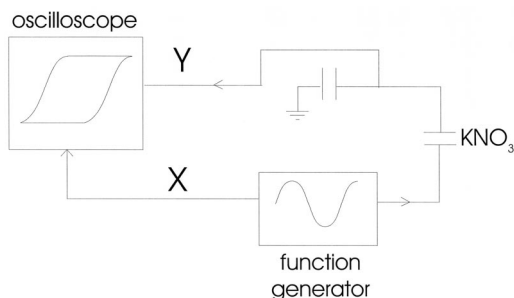


Fig. 3. Sawyer-Tower circuit as implemented in the experimental setup described here.

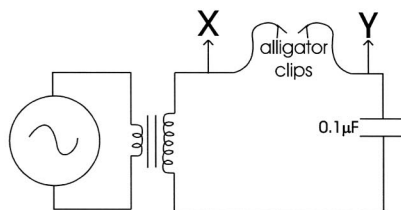
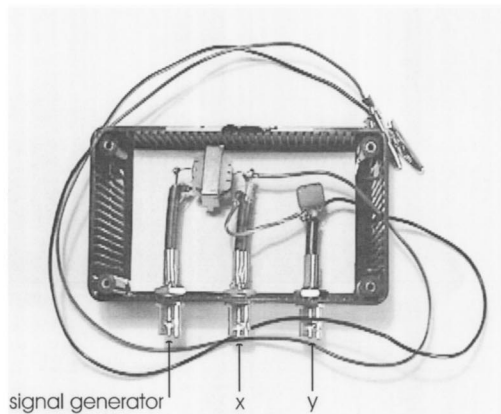


Fig. 4. The test box for the hysteresis measurement. On the left is displayed the actual components; on the right is a diagrammatic representation of the circuit.

By measuring the potential V across a standard capacitor in series with the KNO_3 film one can determine the charge Q on the KNO_3 capacitor using $Q=CV$. When two capacitors are in series the charge on each capacitor must be the same (in an ideal capacitive circuit no current flows), so the electric charges on the standard capacitor and the KNO_3 capacitor are the same. As the capacitance C of the standard capacitor is known we are able to calculate Q from the magnitude of the voltage signal we measure at the standard capacitor.

We display the signal applied to the material as the X signal of an X-Y trace on an oscilloscope. Most of the voltage drops across the KNO_3 capacitor because we have selected a high value of capacitance for the standard capacitor, so we can consider the X signal to represent the voltage across the sample. The Y signal is proportional to the charge on the KNO_3 capacitor.

If this technique were used on an ordinary linear dielectric one would expect a linear response (a straight line on the x-y display), as the polarization is directly proportional to the field applied. In practice there is some opening of the loop, which is due to dielectric loss. In a ferroelectric there is a remnant polarization, i.e., the polarization charge remains aligned in the direction it was poled by the applied field even after this field has been removed. The electrical polarization characteristics of the capacitor thus depend on the history of the field that is applied to it and hence it displays hysteresis.

III. NECESSARY EQUIPMENT

The following equipment is necessary for this experiment:

A. Electrical equipment

- (1) A basic oscilloscope. It must be capable of operating in X-Y mode. It only needs to be capable of operating at low frequencies (100–1000 Hz).
- (2) A signal generator. It should be capable of producing sine waves of 15-V amplitude. Frequencies in the range of 100–1000 Hz give the best hysteresis measurements.
- (3) Hotplate. It should be capable of heating the sample to at least 350 °C. It should be possible to clamp the metal sheet to the edge of the hot plate.
- (4) Thermocouple. A thermocouple is used to measure the temperature of the capacitor during the experiment.
- (5) Test box. A photograph of the test box is shown in Fig. 4. The total cost of the components for this box is very low and it can be assembled easily. The audio transformer

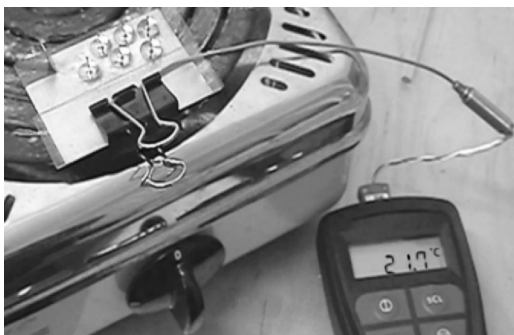


Fig. 5. Assembled experiment before heating. The metal sheet is clamped to the heater between glass slides. The thermocouple is placed below the top slide in contact with the metal sheet. KNO_3 powder is then distributed onto the metal sheet, and thumbtacks are placed on top of the powder.

simply provides more switching voltage. At high frequencies, the signal will become distorted; at the frequencies used in this experiment there is no distortion and this provides an economical way of providing a sufficiently large switching signal. The currents required are tiny. The rest of the circuit is the implementation of the Sawyer-Tower circuit shown in Fig. 3. There are two outputs from the test box. One is the input signal generated by the signal generator after amplification. The other is the signal across the standard capacitor. These are connected to the X and Y channels of the oscilloscope, respectively.

B. Other equipment

In addition to the electrical equipment outlined above, several other items are needed to run the experiment. KNO_3 powder, metal sheeting, e.g., aluminum and copper cut into small squares, and thumbtacks are all used in the experiment as consumables. Students will also require insulated gloves, glass microscope slides, and bulldog clips.

IV. EXPERIMENTAL METHOD

KNO_3 is highly hydrophilic and should be dried before use as the ferroelectricity is degraded when the material has absorbed water. We found that the easiest way to do this was to heat it in a conventional microwave oven for about 2 min. Care must be taken that the powder does not melt in the microwave, as in the molten state KNO_3 is conductive and arcing will occur. After drying, the powder can be stored in a desiccator until needed. KNO_3 is a powerful oxidizing agent, and although the risks of a dangerous reaction are small (we experienced no problems in any of our classes), the KNO_3

should be kept as pure as possible so as to avoid any reactions. In particular it should not be mixed with any carbon-based compound or placed near flames.

As a bottom electrode we used thin aluminum sheeting cut into a square of approximately 25 cm^2 ; a small tab on one corner was bent up to allow easy electrical contact with an alligator clip.

The films are made and measured in the same setup. A hotplate capable of heating to around 350°C is required. Use of a naked flame for heating, such as that from a Bunsen burner, is not recommended because of the potential for ignition of the KNO_3 . The aluminum sheet should be clamped to the hotplate, but must be electrically insulated from it. For this purpose we used bulldog clips and microscope slides. The plate was clamped between glass slides on top and bottom, leaving most of the top surface of the slide exposed. A thermocouple is inserted under the top slide. Once the experiment has been set up as described above a thin covering of potassium nitrate powder should be placed on the bottom electrode. About six to eight thumbtacks should be placed on the powder. We found that upon melting of the KNO_3 , thumbtacks would automatically form a capacitor of suitable thickness; they are also easy to connect to the test box with an alligator clip. The setup of the experiment at this point is shown in Fig. 5.

Once the experiment has been set up the heater should be turned on until the KNO_3 is completely molten. At this point the heater may be turned off and the sample allowed to cool. At about 170°C (above this temperature there is a risk that solder on the clips might melt!) the alligator clips may be attached, one to the bottom electrode and the other to any of the thumbtacks. It is not important which clip is attached to which contact. If at this point a signal is applied, the result on the oscilloscope will be a loop, essentially a linear response opened up by dielectric loss. It is best to apply a 25-V amplitude signal, (full-scale on the X axis for most oscilloscopes) as the coercive voltage for these capacitors is about 17–20 V depending on sample thickness. As the capacitor goes through the phase transition, the loop will change dramatically and become very square. Usually the scale of the Y signal on the oscilloscope needs to be changed. Figure 6 shows a typical result.

Various investigations can be carried out by students. They can easily vary the measurement frequency and assess its effect on remnant polarization and coercive field. The behavior as the temperature continues to fall may also be studied. As the temperature decreases the size of the signal will decrease. We found that 50(60) Hz noise frequently became significant at low signal amplitude. This gives the interested student an additional point of investigation. By selecting applied signal frequencies such as 50(60) and 100(120) Hz, a

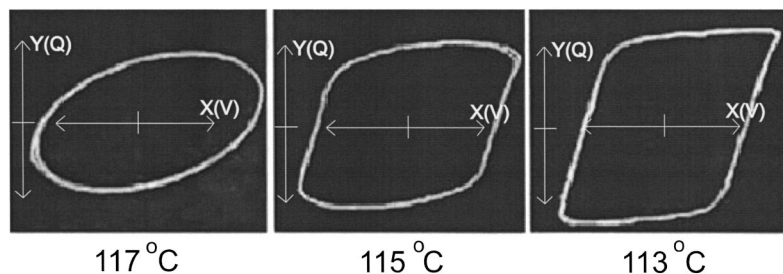


Fig. 6. Typical results seen on the oscilloscope display during the experiment that show the ferroelectric phase transition. The Y signal on the oscilloscope corresponds to the charge on the capacitor Q , while the X signal corresponds to the applied voltage V . Note that for the third picture (113°C) the Y scale on the oscilloscope has been increased as the signal substantially increases when the capacitor undergoes the phase transition, i.e., the charge on the capacitor, Q , increases dramatically after the phase transition occurs.

student can see interference effects between in-phase noise and signal. Many of our students found this the most interesting part of the experiment.

V. CONCLUSIONS

We have developed an experiment to demonstrate ferroelectric polarization hysteresis to undergraduate students. The experiment is simple, safe, and inexpensive. We believe it would complement physics lectures on ferroelectricity or phase transitions in general. It may also be of interest to students studying electrical engineering, materials science, or mineral science. Students get hands-on experience with mak-

ing and characterizing a ferroelectric capacitor. The feedback from students in our course was extremely positive.

¹K. Aizu, "Possible Species of Ferromagnetic, Ferroelectric, and Ferroelastic Crystals," *Phys. Rev. B* **2** (3), 754–772 (1970).

²C. Kittel, *Introduction to Solid State Physics* (Wiley, New York, 1996), 7th ed., Chap. 13.

³E. Fatuzzo and W. J. Merz, *Ferroelectricity* (North Holland, Amsterdam, 1967).

⁴J. F. Scott, *Ferroelectric Memories* (Springer-Verlag, Berlin, 2000).

⁵J. P. Nolte and N. W. Schubring, "Ferroelectricity in Potassium Nitrate at Room Temperature," *Phys. Rev. Lett.* **9** (7), 285–286 (1962).

⁶E. Rapoport and C. G. Kennedy, *J. Phys. Chem. Solids* **26**, 1995 (1965).

⁷J. F. Scott *et al.*, "Properties of ceramic KNO₃ thin-film memories," *Physica B* **150**, 160–167 (1988).

⁸C. B. Sawyer and C. H. Tower, "Rochelle Salt as a Dielectric," *Phys. Rev.* **35**, 269–273 (1930).

Verification of Bohr's frequency condition and Moseley's law: An undergraduate laboratory experiment

S. B. Gudennavar, N. M. Badiger,^{a)} S. R. Thontadarya, and B. Hanumaiah^{b)}

Department of Physics, Karnatak University, Dharwad-580 003, Karnataka, India

(Received 30 August 2002; accepted 28 February 2003)

We describe an undergraduate laboratory experiment to verify Bohr's frequency condition and Moseley's law using a thin NaI(Tl) detector spectrometer and a weak ⁵⁷Co source. The slope of the plot of $K\alpha$ x-ray energy versus $(Z-1)^2$ yields a value for the Rydberg constant, $R = (1.19 \pm 0.01) \times 10^7 \text{ m}^{-1}$, which is in fair agreement with the best literature value, $R = 10\,973\,731.534(13) \text{ m}^{-1}$. © 2003 American Association of Physics Teachers.

[DOI: 10.1119/1.1568969]

I. INTRODUCTION

Several student laboratory experiments on Moseley's law have been described in AJP.^{1–5} All of these experiments, although they are intended for the undergraduate level, involve sophisticated equipment, such as an x-ray machine, an x-ray diffractometer, an electron microscope, Ge(Li) or Si(Li) spectrometers, and intense radioactive sources. Not all undergraduate laboratories can obtain such equipment and also procure radioactive sources with activities of the order of 10^7 Bq. Even if strong sources are procured, they require heavy shielding to protect personnel from radiation. Since Moseley's law should be seen by students at the undergraduate level, it would be desirable to make the experimental arrangement more practicable. In this direction, we have developed a low-cost arrangement that should suit any undergraduate laboratory, including those in underdeveloped countries.

Bohr's theory of atomic structure successfully explains many experimental facts, including the emission of sharp spectral lines. According to this theory, the energy of an electron in its orbit, E_n , is given by

$$E_n = -\frac{R_\infty Z^2}{n^2}, \quad (1)$$

where R_∞ is the Rydberg energy for an infinitely heavy nucleus, Z is the nuclear charge, and $n = 1, 2, 3, \dots$ is the principal quantum number used to designate energy levels. The emission of radiation from the atom, according to Bohr, is due to the transition of the atom from an initial higher energy state (E_i) to a final lower energy state (E_f), and the fre-

quency ν of the emitted radiation is given by the condition $E_i - E_f = h\nu$, where h is Planck's constant. Thus, for instance, $K\alpha$ x-ray emission is due to transfer of an L -shell electron ($n_i = 2$, energy E_L) to the K -shell ($n_f = 1$, energy E_K), where a vacancy has been created by some means (such as by irradiating the atom with γ rays) prior to the transition. Hence the energy of $K\alpha$ x ray is given by

$$E_{K\alpha} = E_L - E_K = \left(-\frac{R_\infty Z^2}{4}\right) - \left(-\frac{R_\infty Z^2}{1}\right) = \frac{3R_\infty Z^2}{4}, \quad (2)$$

which shows that the energy of characteristic x rays is proportional to square of the nuclear charge. In the x-ray notation, the subscript α refers to those transitions of electrons for which $\Delta l = \pm 1$, that is, for electric dipole radiations.

Moseley, who was studying $K\alpha$ x-ray spectra at the same time and in the same laboratory (Rutherford's Manchester Laboratory, Manchester), as Bohr, used this expression, but modified Z to $(Z-1)$ to fit his experimental data. Thus, Moseley used

$$E_{K\alpha} = \frac{3R_\infty (Z-1)^2}{4} \quad (3)$$

to describe his data. Equation (3) is usually referred to as Moseley's law.

In later years, the modification of Z to $(Z-1)$ or $(Z-S)$ was understood in terms of shielding or screening of nuclear charge by the surrounding electrons. So, in the original Moseley's law, the factor $(Z-1)$ means the effective screening for the $K\alpha$ transition is unity.⁶ Thus, from Eqs. (2) and (3) it is clear that various ideas about atomic structure and

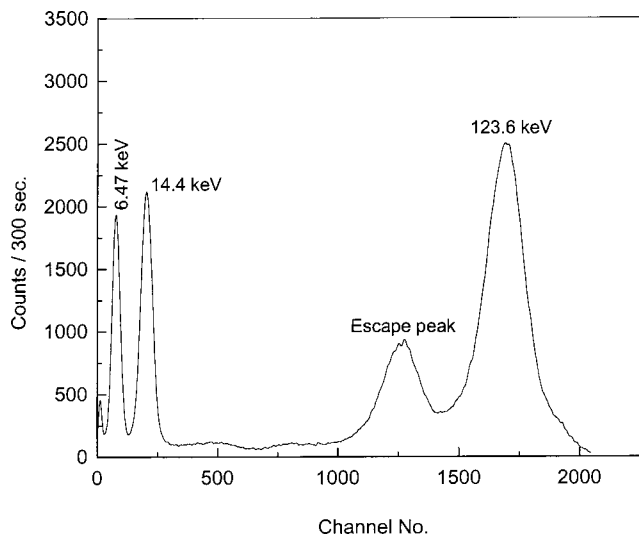


Fig. 1. Spectrum of incident photons from the ^{57}Co radioactive source.

x-ray emission can be verified easily by measuring the energies of characteristic K x rays using a simple x-ray spectrometer.

II. EXPERIMENTAL ARRANGEMENT AND PROCEDURE

The experimental apparatus consists of a low-cost, 1 mm thick \times 38 mm diameter, Bicon NaI(Tl) scintillation detector, a high voltage power supply, a linear amplifier, and a multichannel analyzer (MCA). The x-ray spectrometer is calibrated using several x-ray and low-energy gamma-ray sources that cover the energy range from 6 to 100 keV. A ^{57}Co source of strength of the order 10^4 Bq is employed as the source of exciting radiation. The ^{57}Co nucleus decays by electron capture to ^{57}Fe , emitting 14.4-, 122-, and 136-keV gamma rays, and predominantly emitting the 6.4-keV characteristic $K\alpha$ x rays of ^{57}Fe . The ^{57}Co source has a half-life of 270 days, which is sufficiently long for undergraduate laboratory experiments.

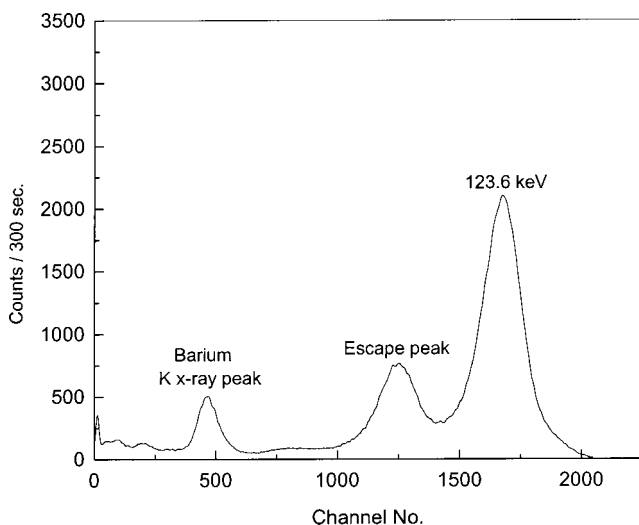


Fig. 2. Spectrum of photons from the ^{57}Co radioactive source that are transmitted through the barium hydroxide compound target.

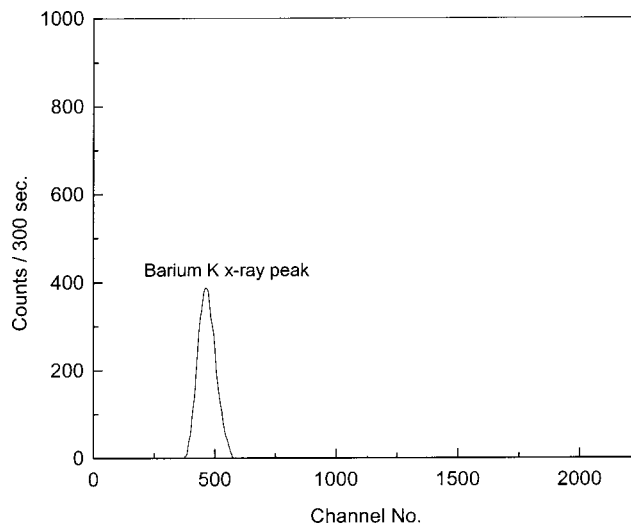


Fig. 3. K x-ray fluorescence spectrum of barium produced by subtracting the incident gamma spectrum from the spectrum of gamma rays transmitted through the barium hydroxide target.

Various targets in elemental and compound form are used to produce characteristic x rays; the compound targets are shaped in the form of pellets. The targets are thin enough to allow the characteristic x rays to pass without much attenuation within the target. There are no other criteria for the targets. We have employed a broad-beam, almost 2π solid-angle configuration, in which the target is sandwiched between the detector and the source. This allows the use of weak radioactive sources.

The procedure to obtain characteristic x-ray peaks is straightforward. First, the incident gamma-ray spectrum is acquired by placing the source very close to the detector. The live time of the MCA is selected to acquire the spectrum. Next, the target is inserted between the source and detector. In this position, gamma rays from the radioactive source excite the characteristic x rays in the target and the characteristic x-ray peak is detected above the transmitted gamma-ray spectrum. Then, the channel number of the x-ray peak can be read out with the help of a cursor. Otherwise, if need be, subtraction of the incident spectrum from the transmitted spectrum yields a clean characteristic x-ray peak from the target. The channel number of the x-ray peak and the corresponding energy are noted. If a printer is available, the printed copies of these spectra can be used for discussion in the classroom.

Typical incident, transmitted, and subtracted spectra for a barium hydroxide target are given in Figs. 1, 2, and 3, respectively. This is repeated for several targets covering the range from $Z=42$ to 82. [For molybdenum, however, the 14.4-keV gamma rays from the ^{57}Co source are attenuated to the level of 10^{-4} using an aluminum block of about 3 mm thickness. This is because the NaI(Tl) detector cannot resolve the 14.4-keV gamma rays and molybdenum K x rays of energy 17.4 keV. If one wants to avoid this difficulty, one can start the sequence with silver ($Z=47$) instead of molybdenum ($Z=42$).] This range of atomic number could be widened by employing a suitable detector, such as HPGe detector, if sufficient funds were available; otherwise, a proportional counter could be used to cover low- and medium- Z targets, while a NaI(Tl) detector would take care of higher Z elements. The NaI(Tl) detector cannot resolve

Table I. Measured and calculated values of the energy $E_{K\alpha}$ for $K\alpha$ x rays of various elements.

Element	Z	Energies of x rays measured with NaI(Tl) detector		Energies of x rays calculated using Eqs. (2) and (3)		Standard literature values
		$(E_{K\alpha\beta})_{\text{obs}}$ (keV)	$(E_{K\alpha})_{\text{der}}^{\text{a}}$ (keV)	$E_{K\alpha}$ (keV)	$E_{K\alpha}$ (keV)	$(E_{K\alpha})_{\text{std}}^{\text{b}}$ (keV)
Mo	42	17.8	17.4	18	17.1	17.442
Ag	47	22.6	22.1	22.5	21.6	22.103
Cd	48	23.7	23.2	23.5	22.5	23.106
In	49	24.7	24.2	24.5	23.5	24.135
Sn	50	25.9	25.3	25.5	24.5	25.192
Ba	56	32.7	31.8	32	30.9	32.017
Pr	59	35.7	34.5	35.5	34.3	35.855
Sm	62	40.3	39	39.2	38	39.910
Gd	64	43.7	42.5	41.8	40.5	42.732
Dy	66	46.9	45.6	44.5	43.1	45.701
Ta	73	58	56.1	54.4	52.9	57.067
Au	79	68.7	66	63.7	62.1	68.120
Pb	82	74.5	71.5	68.6	66.9	74.150

^aUsing Eq. (5).

^bUsing Eq. (6) and Ref. 8.

the $K\alpha$ and $K\beta$ lines, so the K x-ray peak that we obtain is a combination of these K x rays and the peak corresponds to the weighted average energy of the $K\alpha$ and $K\beta$ lines, that is $E_{K\alpha\beta}$. But one can derive the energy of the $K\alpha$ line by using the expression for the weighted average energy,

$$E_{K\alpha\beta} = \frac{K_\alpha E_{K\alpha} + K_\beta E_{K\beta}}{(K_\alpha + K_\beta)} = \frac{E_{K\alpha} + \frac{K_\beta}{K_\alpha} \cdot E_{K\beta}}{\left(1 + \frac{K_\beta}{K_\alpha}\right)} \quad (4)$$

and therefore

$$E_{K\alpha} = E_{K\alpha\beta} + \frac{K_\beta}{K_\alpha} [E_{K\alpha\beta} - E_{K\beta}], \quad (5)$$

where K_β/K_α is the ratio of intensities of $K\beta$ to $K\alpha$ x rays, and $E_{K\beta}$ is the energy of $K\beta$ x rays. Values of K_β/K_α and $E_{K\beta}$ are available in the literature.⁷ For $E_{K\alpha\beta}$, we use our experimental values, denoting them as $(E_{K\alpha\beta})_{\text{obs}}$. Consequently, the derived $E_{K\alpha}$ is denoted as $(E_{K\alpha})_{\text{der}}$, and, in this way, it is our experimental value. We are interested in $E_{K\alpha}$, not in $E_{K\alpha\beta}$, for the present purpose.

III. EXPERIMENTAL RESULTS AND DISCUSSION

In Table I we give the measured energy values of the $K\alpha\beta$ x-ray peaks for various elements. We also give the values of $(E_{K\alpha})_{\text{der}}$, derived from measured values of $(E_{K\alpha\beta})_{\text{obs}}$ using Eq. (5). The values of $E_{K\alpha}$ are calculated using Eqs. (2) and (3), respectively. We give values of $E_{K\alpha}$ obtained by using

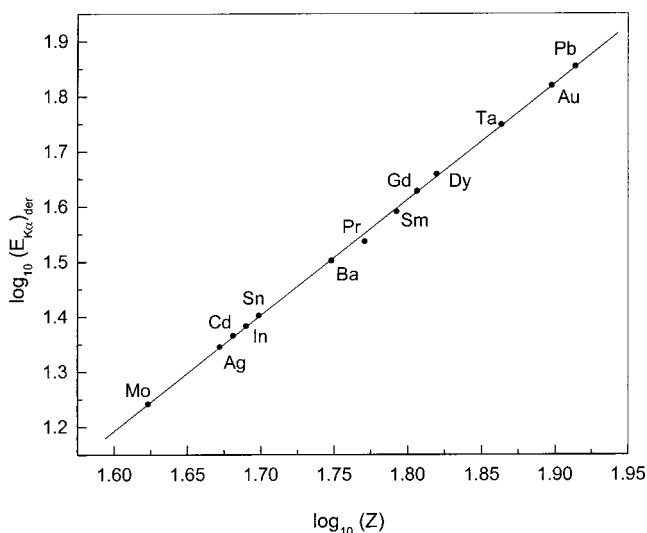


Fig. 4. Dependence of the energy of K x rays on nuclear charge Z and verification of Bohr's frequency condition, Eq. (2) (experimental data, closed circles; least-squares fit, solid line).

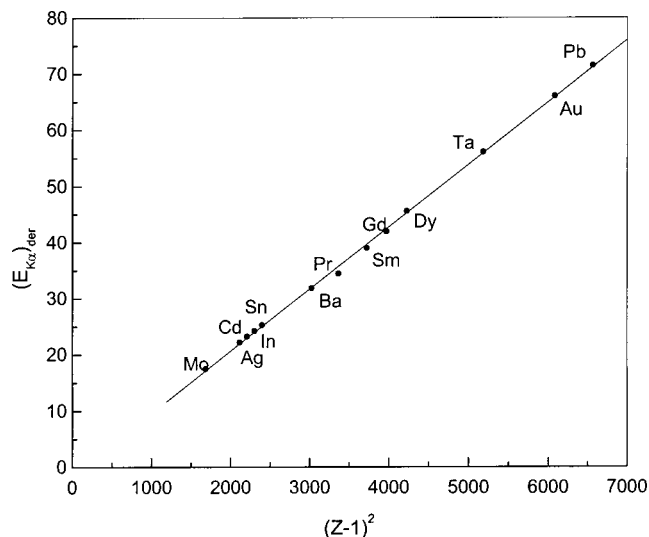


Fig. 5. Moseley plot for elements covering the range $Z=42-82$ (experimental data, closed circles; least-squares fit, solid line).

the ratios of the intensities of $K\alpha 1$ and $K\alpha 2$ lines and their energies $E_{K\alpha 1}$ and $E_{K\alpha 2}$, all of which are available in the literature,⁸ and

$$E_{K\alpha} = \frac{E_{K\alpha 1} + \frac{K_{\alpha 2}}{K_{\alpha 1}} E_{K\alpha 2}}{\left(1 + \frac{K_{\alpha 2}}{K_{\alpha 1}}\right)}. \quad (6)$$

From Table I it is clear that the $E_{K\alpha}$ values obtained from the present experiment are in fair agreement with those calculated using standard values for the energies of the $K\alpha 1$ and $K\alpha 2$ lines. The small deviations of about 5% or less that occur between the two $E_{K\alpha}$ values for Ta, Au, and Pb may be attributed mainly to the deviations of about 3% of the measured values of $E_{K\alpha\beta}$ from the values computed using standard literature values. These deviations are due to the poor resolution of the NaI(Tl) detector and also to uncertainties associated with the $K\beta/K\alpha$ ratios at higher Z values. We see in Table I, that the values of $(E_{K\alpha})_{\text{der}}$ are in fair agreement with the literature values and with the values calculated using Eqs. (2) and (3), although small deviations, especially at higher Z values, are clearly present. These deviations may be attributed to the fact that Bohr's frequency condition corresponds to a single-electron atom and Moseley's modification of Z to $(Z-1)$ is only an approximate way of treating screening in a multielectron atom. Taking these facts into consideration, we can say that the observed values agree fairly well with those calculated using Eqs. (2) and (3). Thus, Bohr's frequency condition and Moseley's law are verified experimentally.

We can display the results graphically and determine R , the Rydberg constant, from the present experiment. In Fig. 4, we plot $\log_{10}(E_{K\alpha})_{\text{der}}$ as a function of $\log_{10}(Z)$. From Fig. 4 we see that the data fall along a straight line with a slope of 2.1, in good agreement with the value 2 expected from Eq. (2). In Fig. 5, we present a Moseley plot for elements in the atomic number range from $Z=42$ to $Z=82$. We see, in Fig.

5, that there is a linear dependence between $(E_{K\alpha})_{\text{der}}$ and $(Z-1)^2$, and from the slope we obtain an experimental value for the Rydberg constant, $R = (1.19 \pm 0.01) \times 10^7 \text{ m}^{-1}$, in fair agreement with the literature value⁹ $10\,973\,731.534(13) \text{ m}^{-1}$ for an infinitely heavy nucleus.

Moseley's law indicates that as one goes from the lighter elements to the heavier elements, the energy of the characteristic x rays emitted from a sample increases in a regular manner and is approximately proportional to $(Z-1)^2$, from which the atomic number Z of a sample can be identified. That is how Moseley was able to identify, from his investigations, the place of Co and Ni, whose atomic weights are in reverse order in the periodic chart.

ACKNOWLEDGMENT

One of the authors (S.B.G.) would like to thank the Karnataka University Dharwad, for the Research Fellowship.

^aElectronic mail: nagappa123@yahoo.co.in

^bPresent address: Vice-Chancellor, Mangalore University, Mangalagangothri-574199, Karnataka, India.

¹C. Hohenemser and I. M. Asher, "A simple apparatus for Moseley's law," *Am. J. Phys.* **36** (10), 882–885 (1968).

²Arthur M. Lesk, "Reinterpretation of Moseley's experiments relating $K\alpha$ line frequencies and atomic number," *Am. J. Phys.* **48** (6), 492–494 (1980).

³P. J. Ouseph and K. H. Hoskins, "Moseley's law," *Am. J. Phys.* **50** (3), 276–277 (1982).

⁴C. W. Haigh, "Moseley's work on x-rays and atomic number," *Am. J. Phys.* **72** (11), 1012–1014 (1995).

⁵C. W. S. Conover and John Dudek, "An undergraduate experiment on x-ray spectra and Moseley's law using a scanning electron microscope," *Am. J. Phys.* **64** (3), 335–338 (1996).

⁶Robley D. Evans, *The Atomic Nucleus* (Tata-McGraw-Hill, Bombay-New Delhi, 1955), pp. 21–22.

⁷James H. Scofield, "Relativistic Hartree–Slater values for K and L x-ray emission rates," *At. Data Nucl. Data Tables* **14**, 121–137 (1974).

⁸N. A. Dyson, *X-rays in Atomic and Nuclear Physics* (Cambridge U.P., Cambridge, 1990), 2nd ed., pp. 378–384.

⁹E. Richard Cohen and Barry N. Taylor, "The 1986 adjustment of the fundamental physical constants," *Rev. Mod. Phys.* **59** (4), 1121–1148 (1987).

A simple vibrating sample magnetometer for use in a materials physics course

Wesley Burgei,^a Michael J. Pechan, and Herbert Jaeger
Department of Physics, Miami University, Oxford, Ohio 45056

(Received 24 June 2002; accepted 14 March 2003)

An inexpensive vibrating sample magnetometer (VSM) has been developed for use in a materials physics course. An exercise using the VSM allows students to measure the magnetic properties of various materials and thus gain experience applicable to contemporary research on magnetic materials. This paper describes specific aspects of the construction of a VSM and presents measurements for two 5-mm-long Ni wires of different diameters and for floppy disk media. A 178- μm -diam Ni wire served as a calibration sample for the system; the results from a 51- μm -diam Ni wire set the limit of precision for this system at approximately 5×10^{-3} emu. © 2003 American Association of Physics Teachers.

[DOI: 10.1119/1.1572149]

I. INTRODUCTION

The vibrating sample magnetometer (VSM), pioneered by S. Foner,¹ is a simple yet effective technique for characteriz-

ing properties of magnetic materials. Due to its straightforward design and continued use among condensed matter physicists and materials scientists, the VSM provides an ideal laboratory exercise for students in an advanced materi-

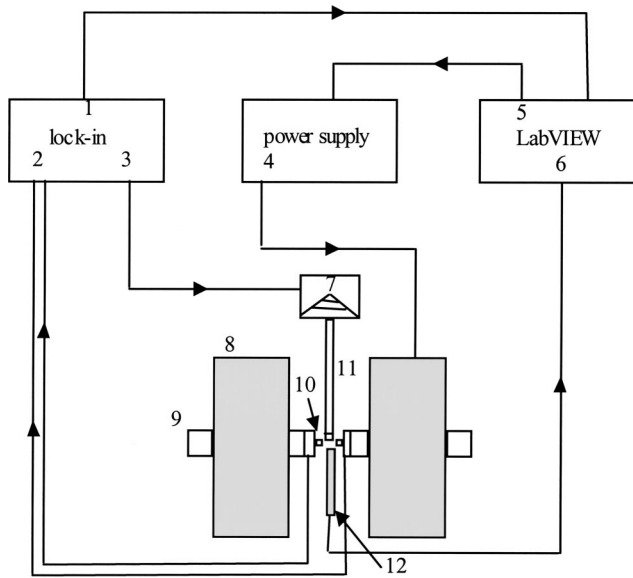


Fig. 1. Schematic diagram of the VSM apparatus showing: (1) coil measurement signal path from the lock-in to LabVIEW via GPIB, (2) signal from the detection coils, (3) driving signal from the lock-in to the mechanical vibrator, (4) the power supply connection to the magnet, (5) the power supply control signal from LabVIEW, (6) the Hall-probe input to LabVIEW via the DAC, (7) mechanical vibrator, (8) electromagnet, (9) magnet pole pieces, (10) detection coil, (11) drinking straw shaft, and (12) Hall probe.

als physics course. This setup allows exploration of a common experimental technique for measuring magnetic material properties such as hysteresis, saturation, coercivity, and anisotropy. The VSM is one of a number of techniques illustrated in our materials physics laboratory course² that emphasizes measurement and characterization of various materials.

Based on Faraday's law of induction, the VSM relies on the detection of the emf induced in a coil of wire given by

$$\varepsilon = -N \frac{d}{dt}(BA \cos \vartheta), \quad (1)$$

where N is the number of wire turns in the coil, A is the coil turn area, and ϑ is the angle between the B field and the direction normal to the coil surface. In practice, knowledge of coil parameters such as N and A is unnecessary if the system can be calibrated with a known sample.

The operation of the VSM is fairly simple. A magnetic sample is placed on a long rod and then driven by a mechanical vibrator. The rod is positioned between the pole pieces of an electromagnet, to which detection coils have been mounted. The oscillatory motion of the magnetized sample will induce a voltage in the detection coils. The induced voltage is proportional to the sample's magnetization, which can be varied by changing the dc magnetic field produced by the electromagnet.

This article focuses on the construction and operation of a relatively inexpensive VSM for a materials physics course. The construction could also serve as a student project. Other than a commercial lock-in amplifier, a variable dc power supply, and a small electromagnet, only inexpensive and readily available components are required for implementation in a teaching laboratory.

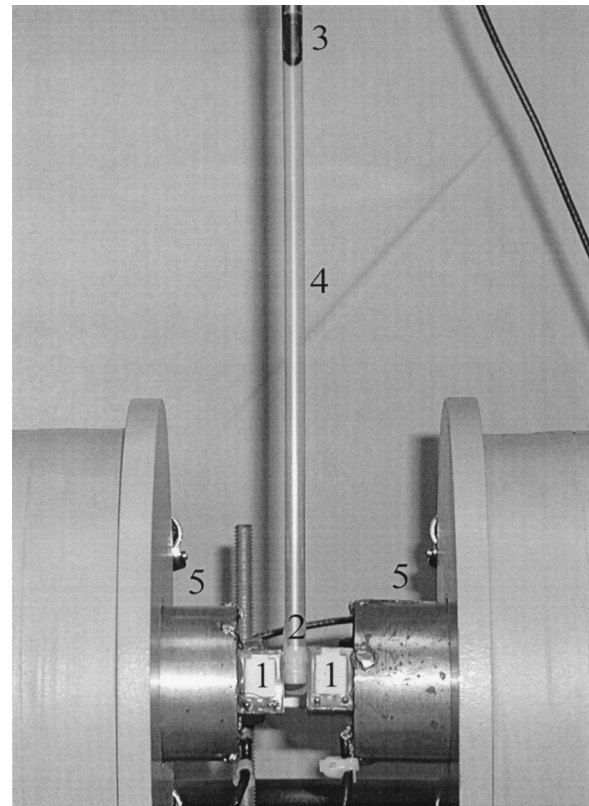


Fig. 2. Photograph of the VSM showing: (1) sense coils, (2) acetal sample mount covered in parafilm, (3) banana plug connector, (4) soda straw sample rod, and (5) magnet pole pieces. The solenoid axis of each sense coil is oriented parallel to the sample rod.

II. APPARATUS

The layout of our VSM is depicted schematically in Fig. 1, and a photograph of the sample rod and pickup coil area is shown in Fig. 2.

A. Oscillating sample mount

Sample oscillation is provided by a Pasco Scientific Model SF-9324 mechanical drive that is mounted to an x - y - z translator³ so that the sample can be centered easily between the magnet poles. The shaft of the sample mount is a long clear drinking straw, which is tightly fitted to the bottom of the mechanical vibrator by a banana plug. We have found that for the intended purposes, the drinking straw provides enough strength and rigidity; however, one could also use a mechanical guide to prevent excess nonaxial motion. An acetal cylinder was machined and fitted inside the bottom of the drinking straw to provide a sample mount. The sample can be fastened with either vacuum grease or a small piece of *Parafilm*[®], the latter being used in our case since the small pole pieces and wide gap produced significant field gradients tending to dislodge the sample. To correct for small variations in vibration amplitude and frequency with time, a reference coil and magnet are often used in research-grade investigations, but they are not employed in the present apparatus.

B. Experimental magnetic field

An air-cooled *GMW*[®] Model 3470 electromagnet with 45-mm-diam pole pieces provides the external applied field. The

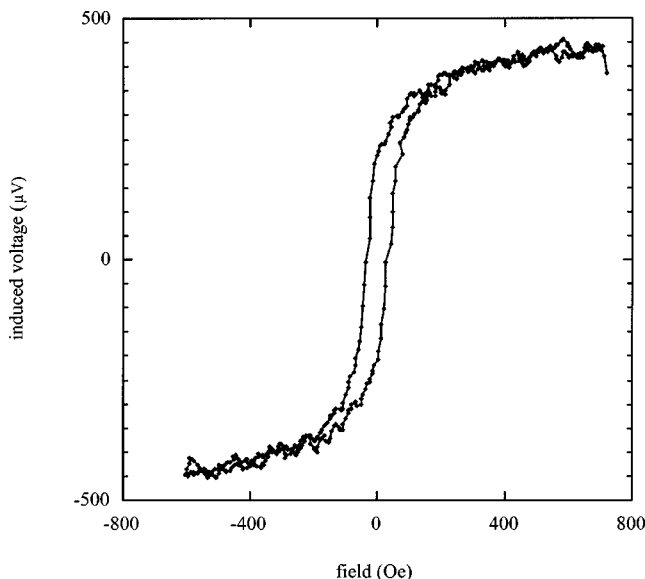


Fig. 3. Hysteresis loop for a Ni wire sample of 5-mm length and 178- μm diameter. This sample is used for magnetization calibration. [To convert to SI units, use 1 oersted (Oe) = $(10^3/4\pi)$ (A/m)].

magnet is powered by a voltage-controlled *Kepeco*[®] 36V/6A bipolar power supply. The magnetic field is measured by an *F.W. Bell*[®] Model 5080 Gauss-meter with analog output capabilities; its Hall probe is mounted between the magnet pole pieces close to the sample position. The electromagnet is attached to a rotating base, which consists of a lazy-susan-type ball bearing rotator and a circular wooden base. This feature allows measurements to be made as a function of angle. As mentioned above, the combination of the small pole-piece diameter and the wide gap necessary to accommodate the detection coils yields a significant magnetic field gradient in the sample region. The field gradient adds noise to the system by introducing a force on the sample that creates nonaxial motion of the straw shaft.

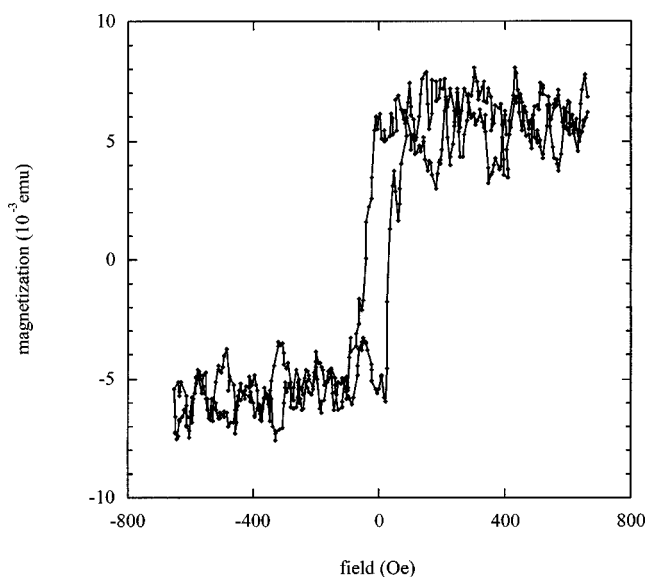


Fig. 4. Hysteresis loop for a Ni wire sample of 5-mm length and 51- μm diameter. This measurement demonstrates the lower level of precision for this system.

C. Signal detection

The most important component that determines the system's resolution is the pick-up coil assembly. While commercial pick-up coils would, of course, provide the highest sensitivity, satisfactory results can be obtained using coils extracted from electro-mechanical relays. In our case, two 32k coils were removed from electromechanical relays;⁴ each coil had an axial length of 18 mm and outer radius of approximately 12 mm. The iron cores of the coils were left in place to increase sensitivity. Each coil was attached with mounting wax to a printed circuit board that was etched with pads for the coil leads and for the coaxial cable running to the lock-in amplifier. The printed circuit board was then attached to the magnet pole pieces so that the cylindrical axis of each pick-up coil was collinear to and coplanar with the axis of sample vibration. The coils are wired so that their induced emfs sum.

Since we are measuring an ac signal and desire to optimize signal-to-noise, we use synchronous detection. We use a *Stanford Research Systems* Model SR830 lock-in amplifier, which is set to lock-on to a signal oscillating at the driving frequency. We use the lock-in amplifier to provide a signal that drives the mechanical vibrator and also serves as the reference signal for the lock-in; however, one could just as easily use a separate function generator for the driving signal and provide it to the lock-in amplifier as a reference signal. It should be noted that if a commercial lock-in amplifier is not available, a less flexible substitute may be constructed using an Analog Devices AD630 balanced mod/demod IC and Burr-Brown's 4423 quadrature oscillator.⁵

D. Automated data collection

A LabVIEW[™] program provides experimental control and data acquisition. The program produces a calibrated analog signal, through a National Instruments Model 6024A data acquisition card (DAQ), which sets the current of the power supply so as to provide the desired magnetic field. The program then sweeps the field from high to low, and then back to high, in steps determined by the user. At each field setting, the induced signal read by the lock-in amplifier is transferred to the computer through the GPIB bus, and the output of the Hall probe is measured through the DAQ. Once the program completes a field cycle, the data are plotted and saved to a text file. All measurements could just as well be made using the DAQ card and analog outputs from the instruments.

III. RESULTS

In our materials physics course, three samples are used to illustrate the VSM technique. Figure 3 shows data from a 5-mm length of 178- μm -diam Ni wire⁶ used for signal calibration. An external field, applied parallel to the sample length, is swept through a complete cycle in order to record a hysteresis loop. Then, using the known Ni magnetization,⁷ 500 emu/cm³, and the known wire volume, we can convert the high field voltage signal (where the magnetization is saturated) into emu units.⁸ (To convert to SI units, use 1 emu/cm³ = 10³ A/m.) Figure 4 shows data from a 5-mm length of 51- μm -diam Ni wire (also with its length parallel to the applied field) that demonstrates the lower limit of resolution of this system is about 5×10^{-3} emu with a signal-to-noise ratio of 3:1. Despite the low signal-to-noise ratio, the magnetic moment of this sample is consistent with that of the

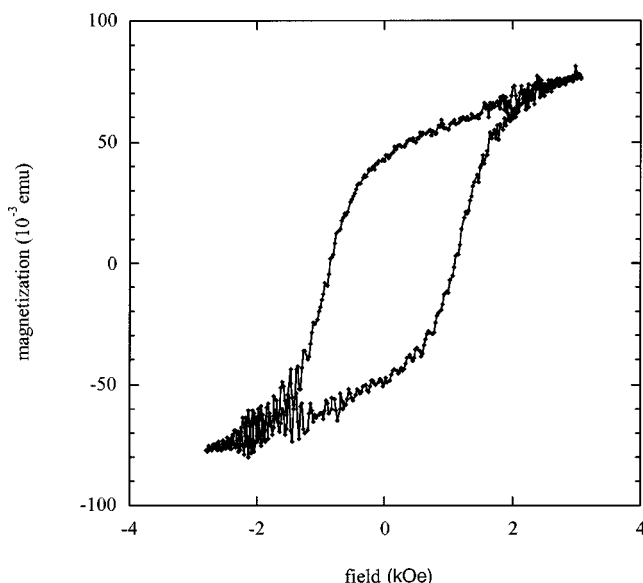


Fig. 5. Hysteresis loop for 5-mm-diameter circular pieces of floppy disk material. Five pieces were stacked together.

178- μm Ni wire if the difference in volume of the two wires is taken into account. Both Ni wire samples exhibit approximately the same coercive field, which is defined as the field producing zero magnetization upon reversal. However, the remnant field—the magnetization in zero field—is quite different for the two. The 51- μm -diam Ni wire is characterized by a square loop with high remnance, implying it has a very abrupt magnetization reversal, whereas the 178- μm sample has lower remnance, consistent with a more gradual reversal process. These results are consistent with shape anisotropy arising from demagnetization effects in a rod-like sample.⁹ Since the length-to-diameter aspect ratio is 3.5 times greater for the 51- μm wire, the shape anisotropy is much greater and therefore more effective in keeping the magnetization along the long axis of the wire. This anisotropy is competing with the randomly oriented crystalline anisotropies associated with the polycrystalline nature of the wire. In the thin wire, the shape anisotropy dominates, whereas in the thick wire, the effect of the randomly oriented crystallites is more evident.

The third sample examined is floppy disk material cut using a hole-punch to make circular pieces with a diameter of 5 mm. Five pieces were stacked together and measurements made with the magnetic field parallel to the planes of the disks. This stack provides a large signal with a good signal-to-noise ratio, as seen in Fig. 5. The resulting hysteresis loop is wide with a relatively high coercivity that is typical of magnetic storage materials. The oscillatory noise at higher fields is due to transverse motion of the sample rod induced by the field gradient.

One could easily investigate the magnetic properties of other readily available samples such as small pieces of paper clip or iron filings.

IV. SUMMARY

The construction and operation of an inexpensive VSM for a materials physics course has been described in detail. Ni wire and floppy disk samples were examined, and, with a magnetization resolution of about 5×10^{-3} emu, this simple VSM provided results that illustrated basic properties of magnetic materials and were suitable for quantitative analysis.

^aElectronic mail: burgeiwa@muohio.edu

¹S. Foner, "Versatile and Sensitive Vibrating-Sample Magnetometer," *Rev. Sci. Instrum.* **30** (7), 548–557 (1959).

²H. Jaeger, M. J. Pechan, and D. K. Lottis, "Materials physics: A new contemporary undergraduate laboratory," *Am. J. Phys.* **66** (8), 724–730 (1998).

³Parts 5200 and 1185, Sherline Products, Inc., 3235 Executive Ridge, Vista, CA 92083-8527.

⁴Part #RTB14730, Schrack Energietechnik GmbH, Seybelgasse 13, 1235 Wien, Austria.

⁵M. J. Pechan, J. Xu, and L. D. Johnson, "Automatic frequency control for solid-state sources in electron spin resonance," *Rev. Sci. Instrum.* **63** (7), 3666 (1992).

⁶California Fine Wire Company, 338 So. Fourth Street, Grover Beach, CA 93433-0199.

⁷Charles Kittel, *Introduction to Solid State Physics* (Wiley, New York, 1986), 6th ed., p. 429.

⁸B. D. Cullity, *Introduction to Magnetic Materials* (Addison-Wesley, Reading, MA, 1972), p. 7.

⁹Reference 8, p. 240.